Brain-computer interface for the epileptic seizures prediction and prevention

1st Vladimir Maksimenko
Innopolis University
Innopolis, Tatarstan, Russia
maximenkovl@gmail.com

2nd Annika Lüttjohann
University of Münster
Münster, Germany

3rd Sabrina van Heukelum
Radboud University
Nijmegen, The Netherlands

4th Janita Kelderhuis
Radboud University
Nijmegen, The Netherlands

5th Vladimir Makarov
Innopolis University
Innopolis, Tatarstan, Russia

6th Alexander Hramov
Innopolis University,
Innopolis, Tatarstan, Russia

7th Alexey Koronovskii
Saratov State University
Saratov, Russia

8th Gilles van Luijtelaar
Radboud University
Nijmegen, The Netherlands

***Abstract*—30% of epileptic patients are resistant to drug therapy. A prospective treatment strategy for refractory epilepsy patients is a brain-computer interface (BCI) in which the epileptic seizures are modulated either by the preprogrammed stimulation schedules (open loop) or via the closed-loop stimulation. The closed-loop BCI implies that seizures are automatically detected and that the detection triggers stimulation which subsequently aborts seizures. Up to now, this experimental treatment is only able to reduce seizures duration, while the ultimate aim is their complete abolishment. We have developed a closed-loop BCI aimed to predict and prevent spike-wave discharges, the electrophysiological anchor of absence seizures, in a genetic absence rat model; it predicted 45% of the seizures while the remaining ones were detected. When we evaluated the combination of the prediction and seizure detection with closed-loop electrical stimulation, a 72% decrease of seizure activity duration was achieved.**

***Index Terms*—brain-computer interface, seizure prediction, brain stimulation**

I. Introduction

Epilepsy is a neurological disease characterized by spontaneous seizures. At the moment, around 50 million people in the world suffer from different types of epilepsy. Epileptic seizures are associated with the formation of patterns of rhythmic brain activity, involving neural populations located in different brain areas. One of the most common ways to prevent epilepsy is to use medical drugs. These medications affect through a variety of mechanisms, often acting to suppression channels. Although the development of antiepileptic drugs began more than 20 years ago, so far one-third of patients are not amenable to this type of treatment. For these patients, it seems effective to use the brain-computer interface (BCI) based on the destruction of pathological neural activity by the stimulation [1]. At the moment, several methods allow effective suppression of epileptic seizures using electric [2], magnetic [3] and optogenetic stimulations [4].

The stimulation can be activated following the predetermined stimulation protocol without analyzing brain activity. This action is the characteristic feature of the open-loop control using an antiepileptic device. This means that there is no direct feedback between the brain state and the stimulation protocol [5].

It is obvious that to be more effective, the stimulation should be performed following the peculiarities of the current brain state. It can be implemented in the BCI operating on the principle of closed-loop control, where the monitoring of the brain state is carried out using the signals of electrical brain activity. One of the first "closed-loop" clinical trials, was the responsive neurostimulator (RNS) designed by Neuropace Inc. (CA, USA) [6]. It contained implanted electrodes for recording the intracranial EEG served as an input for the algorithm which determined when a seizure has started. The triggered focal electrical stimulation was sent to a specific brain area to interrupt the seizure.

The further development of antiepileptic BCIs should be aimed at a search of biomarkers of neural activity, allowing to predict the occurrence of epileptic seizures, as well as a search for the most effective stimulation parameters for the destruction of pathological activity with the least impact on the normal brain functioning [1]. Although algorithms are enabling the seizure detection with the high sensitivity and specificity [7], the prediction of the seizures is a more challenging task, since the preictal activity might not differ from the normal behavior. For instance, the developed algorithms can predict seizures with a high sensitivity but their specificity is too low to be used in clinics [8]. According to the recent works [9], [10], the development of efficient systems for predicting epileptic seizures remains a challenging task of modern neuroscience.

To address this issue we propose a closed-loop BCI for the seizure prediction and prevention and test it in-vivo in rats. The developed BCI correctly predicts 45% seizures and the number of false predictions varies from 20 to 100 per hour for the different animals. Finally, having evaluated the proposed BCI, a 72% decrease in seizure activity duration has been achieved.

978-1-7281-4707-9/20/$31.00 ©2020 IEEE

II. METHODS

A. Animals

Male 6–7 months WAG/Rij rats (body weight ca 354 gr) were used as experimental subjects. The rats were born and raised at the department of Biological Psychology, Donders Centre for Cognition, Radboud University Nijmegen, the Netherlands. Before surgery they were housed in pairs, after surgery they were singly housed (High Makrolon cages with Enviro Dri bedding material and cage enrichment). Rats were always kept on a 12:12 light cycle (light off phase between 8.30 h and 20.30 h), with food and water ad libitum. All efforts were done to restrict the number of rats and to make the discomfort for the rats as minimal as possible. All procedures were carried out in accordance with the Ethical Committee on Animal Experimentation of Radboud University Nijmegen (RU-DEC).

B. Surgery

The stereotactical surgery was performed under isoflurane anesthesia. All rats were implanted with a tripolar electrode set (Plastic One MS 333/2a) and two bipolar electrode sets (Plastic One MS 303/11). All electrode sets consisted of stainless steel wires, isolated with polyimide, diameter 0.2 mm. Only the tip of each electrode wire was un-isolated. The first electrode set comprised a thalamic (A/P: -3.6 mm, M/L: -2.4 mm, H: 6.4 mm) EEG electrode, and a reference and earth to the cerebellum. The first bipolar electrode was used to record the EEG in layer 5/6 of the somatosensory cortex ((A/P: both electrodes -0.5, M/L: 4.5 and 5.0, H: 4.5 and 5.0), the second electrode set was a bipolar stimulation electrode , coordinates were A/P: 2.0 mm, M/L: 4.4 mm, H: 4.1 mm and A/P: -3.0 mm, M/L: 4.8 mm, H: 2.95 mm. All coordinates were according the stereotactic atlas of Paxinos and Watson (1998). The electrodes were fixed to the skull with dental cement (Simplex Rapid, Kemdent, Purton, Swindon, Wiltsher, UK). The animals received injection with Atropine (0.05 ml intramuscular) and Rimadyl (0.14 ml subcutaneous) preoperative and postoperative Rimadyl (24 and 48 hours after surgery, 0.14 ml subcutaneous). Rats were allowed 14 days recovery before any electrophysiological experiments were performed.

C. ECoG recording

Rats were habituated to the Plexiglas recording cage (20x35x25 cm) and cables for at least 16 hours: the leads were attached to a swivel-contact to allow registration and stimulation in the freely moving animal. A physiological amplifier (TD 90087, Radboud University, Nijmegen, Electronic Research Group) amplified the EEG signals which were filtered by a band pass filter with cut-off points at 1(HP) and 100(LP) and a 50 Hz Notch filter. Differential EEG recordings were made form the two cortical sites and the thalamus. The EEG signals were digitalized by WINDAQ-recording-system (DATAQ-Instruments Inc., Akron, OH, USA) with a constant sample rate of 500 Hz. A Passive Infrared Registration (PIR) system registered the movements of the rat (RK2000DPC LuNAR PR Ceiling Mount, Rokonet RISCO Group S.A., Drogenbos, BE). The EEG was recorded for a base-line period between 9.00 and 16.00, next the threshold for electrical cortical stimulation for SWD interruption was determined by finding the intensity at which three subsequent SWD were aborted by the 1 sec train 130 Hz pulses. This intensity was used in the seizure prevention experiment.

D. ECoG analysis

The time-frequency decomposition of the each ECoG signal $X_i(t)$ was performed using a continuous wavelet analysis

$$A_i(s,t) = \frac{1}{\sqrt{f}} \int_{t-s}^{t+s} X_i(t')\psi^*(\frac{t-t'}{s})dt', \qquad (1)$$

with the specially designed mother complex function

$$\psi(\eta) = \pi^{1/4}\mathrm{Exp}[\mathrm{i}\omega_0\eta]\mathrm{Exp}\left[\frac{-10\eta^4}{2}\right], \qquad (2)$$

where $s = 1/f$ [Hz^{-1}] is the timescale, f is the linear frequency [Hz]. The used mother wavelet function is the modification of the well-known Morlet wavelet [11]. The power spectrum $W_i(s,t) = |A_i^2(s,t)|$ was calculated during a 600-ms window for the frequency range 3-20 Hz. The algorithm was implemented in real time with the time step $\Delta t = 0.005$ s – small enough to provide high-quality signal decomposition in the considered frequency range. The resulted measure $W(s,t)$ was found as a product of the spectra obtained for the all ECoG recordings $W(s,t) = W_1(s,t) \times W_1(s,t) \times W_1(s,t)$ at the every moment of time. The values $W_{\Delta s_j}(t)$, corresponding to the spectral energy of the timescales Δs_j, were given by the equation

$$W_{\Delta s_j}(t) = \frac{1}{\Delta s_j} \int_{s\in\Delta s_j} \frac{1}{\tau} \int_{t-\tau}^{t} W(s,t_0)dsdt_0, \quad j = \overline{1,3}, \quad (3)$$

where the integration was performed both over the range of timescales and the time interval $\tau = 500$ ms chosen experimentally considering the minimal duration of the precursor.

E. Seizure prediction

In order to automatically recognize the precursor and to reduce the number of false alarms caused by any other patterns of synchronized neuronal activity, the three ranges of timescales corresponding to the common patterns of synchronic neuron activity: Δs_1 (the range of sleep spindles 7–20 Hz), Δs_2 (the range 5–10 Hz of theta/alpha–precursors), Δs_3 (the range of low-frequency oscillations (delta-precursors) 3–5 Hz) were considered [12]. For these ranges the values of mean energy (3) were calculated

In Fig. 1, b the rectangular windows, each of length τ and width Δs_1 ,Δs_2 , Δs_3 shown by the dotted, solid and dashed lines, respectively, correspond to the areas of values on the time-frequency plane (s,t) over which $W_{\Delta s_{1,2,3}}(t)$ are calculated at the moment of time $t = t^*$. During the online calculation the current moment of time t was located at the

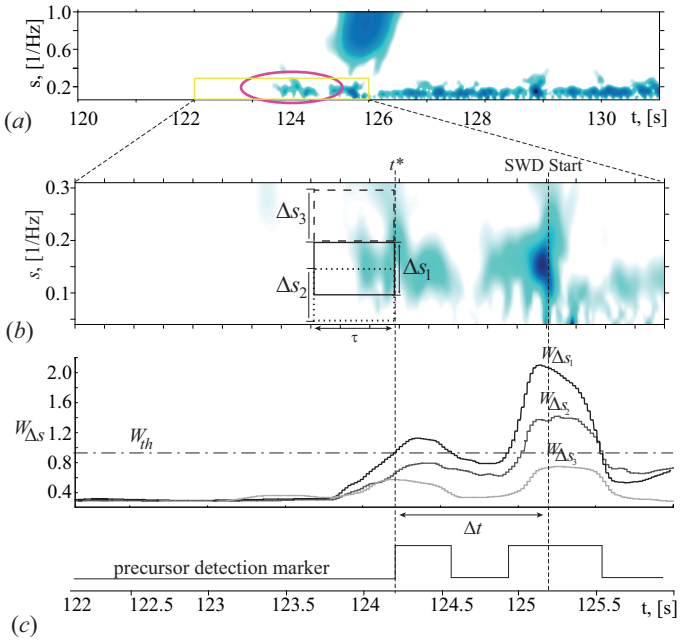

Fig. 1. The range of the timescales, corresponding to the preictal period and SWD onset is shaded (a). A detailed illustration of the surface $W(s,t)$ preictally and during SWD onset (b). The rectangular windows correspond to the areas of parameters (s,t), for which the value of $W(s,t)$ is averaged. (c) The values $W_{\Delta s_i}$ in every moment of time correspond to the $W(s,t)$, averaged over the rectangle of the width Δs_i, respectively. W_{th} is the threshold energy value, used for the prediction. Δt is the time between the detected precursor activity and the onset of SWD.

right-hand side of a rectangles, so, the algorithm stored half of second prehistory and used it for averaging. Since the new amount of data came from the hardware the rectangles shifted to the right with the step $\delta t = 1/SR$, where $SR = 200$ Hz is the sample rate, and the quantities $W_{\Delta s_{1,2,3}}(t)$ were then calculated for the next moment of time. In Fig. 1 one can see that value of the mean energy $W_{\Delta s_2}(t)$ during the precursor activity becomes larger than $W_{\Delta s_{1,3}}(t)$ and, moreover, exceeds the same value corresponding to the background activity. So, setting the threshold value W_{th} we can automatically detect the precursor with the help of three conditions:

- condition 1: $W_{\Delta s_2} > W_{\Delta s_{th}}$;
- condition 2: $W_{\Delta s_2} > W_{\Delta s_3}$;
- condition 3: $W_{\Delta s_2} > W_{\Delta s_1}$.

The conditions (2) and (3) were used to distinguish the precursor events from sleep spindles and low-frequency delta activity. Similar to the seizure, these types of activities are also induced by synchronous neuronal dynamics, but have higher (up to 20 Hz) and lower (up to 5 Hz) frequencies, respectively.

F. stimulation

The stimulus generator was controlled by the custom software, allowed to read and apply the set of the pulse parameters (e.g. duration, frequency, intensity) from a text file . In order to minimize the idle time, once the precursor was detected, the prediction algorithm immediately activated the additional thread responsible for the establishment of the connection with the stimulator and sending a precursor detection marker. The precursor detection marker was a s pulse sent to the Acquisition hardware via the LPT-port. The thread existed for one second and blocked the signals coming from the prediction algorithm. It prevented the rat from an additional stimulation caused by the artifacts that appeared in the cortical EEG during the delivery of the first pulse train.

G. Estimation of the brain response

III. Results

At the first step the prediction algorithm was implemented by comparing the wavelet spectral energy in the 5–10 Hz frequency band with the predefined threshold (condition 1). The algorithm's seizure prediction performance was evaluated with EEG recordings (four hours in duration) of WAG/Rij rats. It was found that the algorithm correctly predicted on average 88% of the SWD (Fig. 2, a). For the individual animal this value varied in the range 80–100% (Fig. 2, b), The remaining SWDs were (early) detected. At the same time, a high number of false positive predictions was noticed; they mainly occurred during light slow wave sleep, a state of alertness, in which neurons are slightly hyperpolarized and at high risk for seizure generation. Only few false alarms were generated during active wakefulness, passive wakefulness and deep slow wave sleep (Fig. 2, e). Despite the high sensitivity of the algorithm, it was not implemented in the closed-loop stimulation to prevent the rat against the large number of false stimulations.

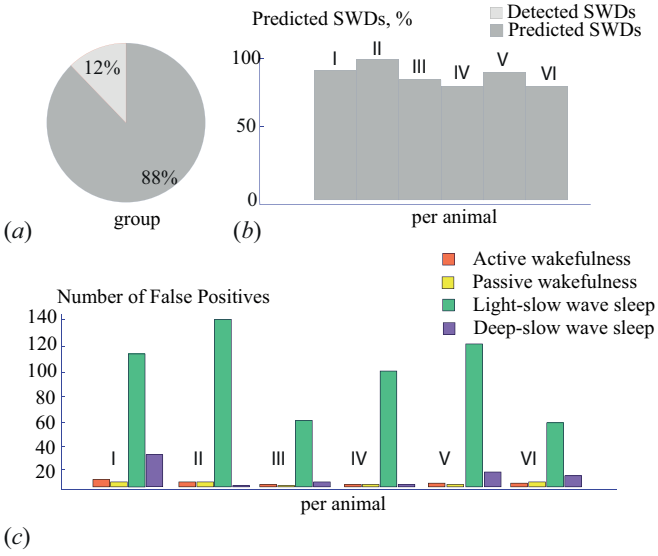

Fig. 2. Percentage of predicted and detected SWDs within the 4 hours recording of the group of six WAG/Rij rats (group (a) and individual (b) data). (c) number of false positives across different states of alertness. For each rat and each state of alertness, 5 segments of 50 seconds duration were randomly selected in each recording for quantification of the number of false alarms.

At the second step the prediction algorithm was extended to reduce the number of false positives. The extension was based on the simultaneous consideration of the wavelet energies of two other frequency bands, associated with synchronized brain

activity: Δs_2 (7–20 Hz, the range of sleep spindles, which in rats have a broad frequency spectrum), and Δs_3 (the range of low-frequency oscillations (high (3–5) Hz delta, light slow wave sleep). The precursors were now automatically detected with the help of a set of logical conditions (for details see the Methods section and Fig.1). This resulted in a significant reduction of the false alarm rate of 83%±3.3% ($F(1,10) = 321.35, p < 0.001$) (Fig. 3, a). As the result, the number of false detections varied from 10 to 130 per hour (Fig. 3, b). The mean percentage of the predicted SWDs was decreased to 45% when compared to the initial version (Fig. 3, a). At the same time, for 4/6 animals the percentage of predicted SWDs exceeds 50% (Fig. 3, d).

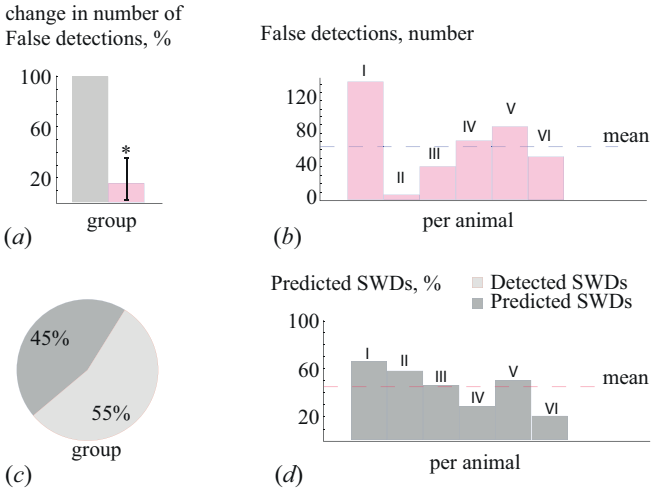

Fig. 3. (a) the relative decrease in the false positives rate (left pannel) between the first algorithm (gray) and the second algorithm (red). (b) number of false positives for each individual rat generated by the revised algorithm within the 1 hour baseline of the 6 WAG/Rij rats. (c) mean and (d) individual percentage of correctly predicted and correctly detected SWDs by the algorithm including two additional critera (conditions 2 and 3). The data are from an one hour baseline recording of 6 WAG/Rij rats.

Finally, the latter version of the prediction algorithm was implemented in a closed-loop deep-brain stimulation system. In this system the ECoGs of freely moving rats, recorded from two cortical and a thalamic site, were fed via an amplifier to a data acquisition system. They were analyzed in terms of synchrony in real time by the prediction algorithm. Whenever the level of synchrony exceeded a preset threshold value (condition 1), and the two other criteria (conditions 2 and 3) were met (see Methods for details), a marker was set in a free channel of the acquisition system and a constant current stimulator was triggered to deliver a low intensity 1 sec pulse train of 130 Hz to the rat. The wavelet energy within this frequency band drastically dropped during and following 130 Hz stimulation, indicating that this electrical pulse train efficiently desynchronized the EEG and thereby successfully prevented the generation of a hypersynchronous SWD (Fig. 4).

The preset detection threshold value was determined for each individual rat and varied between 0.10 and 0.40. We assumed that a pulse train of 130 Hz should prevent SWDs. This assumption was based on our previous work, in which it

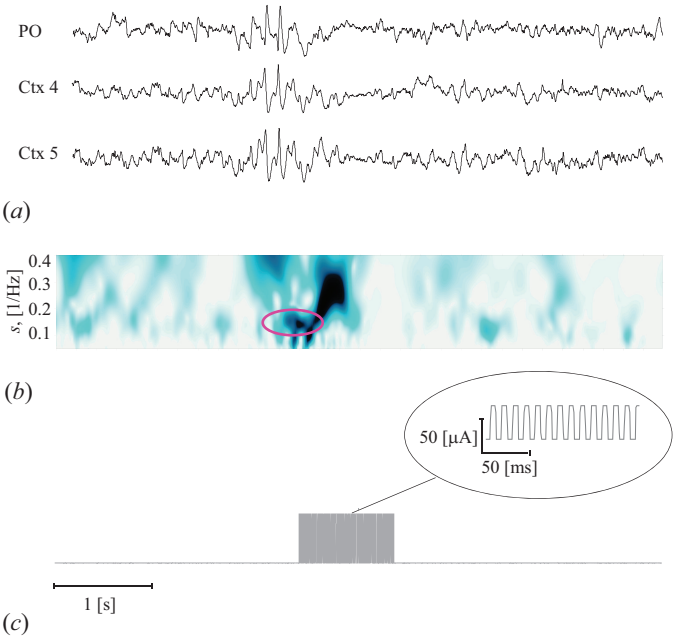

Fig. 4. The seizure prevention by means of electrical stimulation with the pulse duration: the EEG signals, taken from postero/lateral thalamus (PO) and cortex layers 4 and 5 (a), the distributions of the wavelet energy $W(s,t)$ (b) and the pulse train (c) (the structure of pulse is also shown in detail).

was established that this pulse train was rather effective (close to 90%) in interrupting ongoing SWDs. A comparison of SWD activity between an one hour baseline recording in which no stimulation was applied, and SWD activity during an one hour stimulation session showed that SWD activity was reduced by 72±10% ($F(1,5) = 48.52, p < 0.001$) (Fig.5, a). The reduction in SWD activity can be attributed to a combination of SWD prediction and prevention (in 45% of cases) and SWD detection and interruption. To support the conclusion that the reduction was not just the result of detection and disruption, we refer to the individual data of two rats in whom seizures were reduced by 98% and 100%, showing that total prevention of SWD activity by prediction and stimulation is feasible.

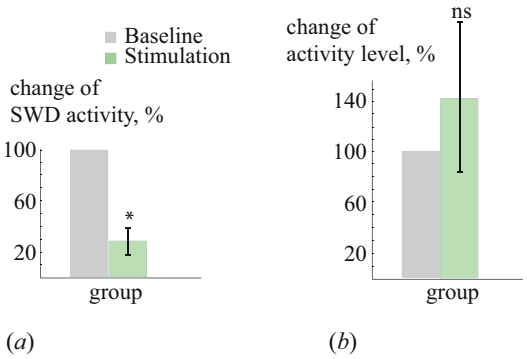

Fig. 5. The total duration of the epileptic activity(a) and the behavioral activity (b) during the baseline and the stimulation session, averaged over the group of rats. The error bars show the standard error of the mean of the group.

In order to establish whether the remaining false positive

detections, which also triggered the delivery of the electrical pulse train, might have affected the behavior of the animals, we compared the activity of rats between baseline and stimulation hour. The behavioral activity was measured by a passive infrared registration (PIR) device. There was no significant difference in activity of the rats between the baseline and stimulation session (Fig. 5, b) $(F(1,5) = 0.476, p = 0.521)$, suggesting that the decrease in SWD activity induced by stimulation cannot be explained by an increase in behavioral activity. It is well known that motor activity precludes the occurrence of SWDs. Furthermore, no other type of aberrant activity was observed in the EEG recordings of the animals during or after stimulation, and given the low intensity of electrical stimulation to prevent and disrupt SWDs and the relatively short stimulation trains, we presume that this type of stimulation can be considered a relatively safe intervention strategy.

IV. Conclusion

The developed BCI can be considered as a step toward closed-loop antiepileptic devices enabling the complete seizure abolishment in drug-resistant patients. The developed BCI has high efficiency in reducing not only the duration of epileptic seizures but also their number. At the same time, the further use of the BCI to control epileptic activity in humans is limited due to a large number of false detection. Despite the fact that additional stimulation did not cause changes in animal activity, the safety of using BCIs for people requires further efforts to increase the prediction selectivity and reduce the number of false detections.

Acknowledgment

This work has been supported by the Center for Technology in Robotics and Mechatronics Components (Innopolis University).

References

[1] W. C. Stacey and B. Litt, "Technology insight: neuroengineering and epilepsy—designing devices for seizure control," *Nature Reviews Neurology*, vol. 4, no. 4, p. 190, 2008.

[2] A. L. Velasco, M. Velasco, F. Velasco, D. Menes, F. Gordon, L. Rocha, M. Briones, and I. Márquez, "Subacute and chronic electrical stimulation of the hippocampus on intractable temporal lobe seizures: preliminary report," *Archives of Medical Research*, vol. 31, no. 3, pp. 316–328, 2000.

[3] V. K. Kimiskidis, D. Kugiumtzis, S. Papagiannopoulos, and N. Vlaikidis, "Transcranial magnetic stimulation (tms) modulates epileptiform discharges in patients with frontal lobe epilepsy: a preliminary eeg-tms study," *International journal of neural systems*, vol. 23, no. 01, p. 1250035, 2013.

[4] E. Krook-Magnuson, C. Armstrong, M. Oijala, and I. Soltesz, "On-demand optogenetic control of spontaneous seizures in temporal lobe epilepsy," *Nature communications*, vol. 4, p. 1376, 2013.

[5] M. Hodaie, R. A. Wennberg, J. O. Dostrovsky, and A. M. Lozano, "Chronic anterior thalamus stimulation for intractable epilepsy," *Epilepsia*, vol. 43, no. 6, pp. 603–608, 2002.

[6] E. H. Kossoff, E. K. Ritzl, J. M. Politsky, A. M. Murro, J. R. Smith, R. B. Duckrow, D. D. Spencer, and G. K. Bergey, "Effect of an external responsive neurostimulator on seizures and electrographic discharges during subdural electrode monitoring," *Epilepsia*, vol. 45, no. 12, pp. 1560–1567, 2004.

[7] A. Ovchinnikov, A. Lüttjohann, A. Hramov, and G. Van Luijtelaar, "An algorithm for real-time detection of spike-wave discharges in rodents," *Journal of neuroscience methods*, vol. 194, no. 1, pp. 172–178, 2010.

[8] G. van Luijtelaar, A. Lüttjohann, V. V. Makarov, V. A. Maksimenko, A. A. Koronovskii, and A. E. Hramov, "Methods of automated absence seizure detection, interference by stimulation, and possibilities for prediction in genetic absence models," *Journal of neuroscience methods*, vol. 260, pp. 144–158, 2016.

[9] L. Kuhlmann, K. Lehnertz, M. P. Richardson, B. Schelter, and H. P. Zaveri, "Seizure prediction—ready for a new era," *Nature Reviews Neurology*, vol. 14, no. 10, pp. 618–630, 2018.

[10] D. R. Freestone, P. J. Karoly, and M. J. Cook, "A forward-looking review of seizure prediction," *Current opinion in neurology*, vol. 30, no. 2, pp. 167–173, 2017.

[11] A. E. Hramov, A. A. Koronovskii, V. A. Makarov, A. N. Pavlov, and E. Sitnikova, *Wavelets in neuroscience*. Springer, 2015.

[12] V. A. Maksimenko, S. van Heukelum, V. V. Makarov, J. Kelderhuis, A. Lüttjohann, A. A. Koronovskii, A. E. Hramov, and G. van Luijtelaar, "Absence seizure control by a brain computer interface," *Scientific Reports*, vol. 7, no. 1, p. 2487, 2017.